This article has been accepted for publication in a future issue of this journal, but has not been fully edited. Content may change prior to final publication. Citation information: DOI 10.1109/TSTE.2018.2884699, IEEE Transactions on Sustainable Energy

Wind Turbine Power Curve Modeling and Monitoring with Gaussian Process and SPRT

Peng Guo, David Infield

***Abstract*-- The wind turbine power curve is an important indicator of the performance of a wind turbine. Modeling and monitoring the power curve can detect wind turbine operating abnormalities and degradation in a timely manner. This paper firstly points out the drawbacks of the standard binned power curve modeling method of IEC-61400-12-1. Multiple factors that influence the wind energy capture and power output of a wind turbine are analyzed in detail and used as the power curve model inputs. A multivariable power curve model is constructed with a modified Cholesky decomposition Gaussian Process (GP) and validated using wind turbine SCADA data. A Sequential Probability Ratio Test (SPRT) with two groups of hypotheses is introduced to analyze and detect abnormal changes in GP power curve prediction residuals and thus detect abnormal operation. In order to locate failed components when an alarm is identified, longitudinal and transverse data comparisons are proposed to check the operation of specific components. The modeling and monitoring methods proposed in this paper successfully identify faults and locate the faulty component for two wind turbines with anemometer failure and pitch system failure respectively.**

***Index Terms*-- wind turbine power curve, condition monitoring, Gaussian Process (GP), Sequential Probability Ratio Test (SPRT), data comparison.**

I. Introduction

The wind turbine power curve is an important indicator of wind energy capture efficiency and power generation performance. Modeling and monitoring the wind turbine power curve can detect early abnormalities and failures in a timely way so that the availability of the wind turbine can be improved and the maintenance cost decreased. In IEC standard IEC61400-12-1 [1], ten minute interval sampled wind speed and power data are used to create the power curve by calculating mean values of the wind speed and power in different wind speed bins. The authors of [2] and [3] have provided a good overall review of wind turbine power curve modeling methods. In [4-5], parametric models such as the logistic function and non-parametric models such as multi-layer perceptron (MLP) and random forests have been used to model the power curve and results of different methods are compared with each other. In [6], four nonlinear parameter models including a six-order polynomial regression function and a hyperbolic tangent function are used to model the power curve. The above power curve modeling methods only use the wind speed as the model's input, and other factors known to influence power output are not considered. In [7], the authors propose a method to improve power curve modeling accuracy by using a turbulence intensity correction. Because wind turbines in downwind rows are impacted by the wakes of upstream turbines, performance differences between wind turbines are created. [8] adds wind direction to the power curve model and gets improved model accuracy. These two papers use additional input parameters in their power curve models but do not give an overall analysis of the factors that influence wind turbine power output.

In this paper, the binned power curve modeling method of IEC61400-12-1 is introduced and its drawbacks pointed out in Section 2. In Section 3, the factors which have influence on wind turbine power are analyzed in detail and out of this a multivariable input power curve model is constructed using a modified Gaussian Process approach. Finally, a Sequential Probability Ratio Test (SPRT) method is used to analyze the power curve model prediction residuals and generate wind turbine operational alarms in Section 4. With two wind turbine study cases, one for anemometer failure and another for pitch failure, the power curve modeling and monitoring method proposed in this paper is proved to be effective.

II. Binned Power Curve Construction Method and Its Drawbacks

IEC standard IEC61400-12-1 describes power curve modeling using the so called "method of bins". The bins method uses the 10-minute wind speed and power output data to generate a power curve. The bins method divides the wind speed range from 0m/s to cut-out wind speed (usually 25m/s) into 0.5m/s intervals (known as bins) and calculates the mean values of the wind speed and power output for each wind speed bin. The power curve comprises some pairs mean wind speed and power output values which reflect the mean power output in the different wind speed bins.

The method of bins for power curve modeling is highly effective in terms of data reduction and ease of calculation. But it has drawbacks and limitations as follows:

(1) The bins method uses just the mean wind speed and power output to represent the N_i data points (the wind speed and power output of each record make one data point) within wind

This work was supported in part by the National Natural Science Foundation of China under Grant 51677067.

Peng Guo is with the School of Control and Computer Engineering, North China Electric Power University, Beijing, 102206, P. R. China (e-mail: pengguo@ncepu.edu.cn).

David Infield is with the Institute of Energy and Environment within the Department of Electronic and Electrical Engineering, University of Strathclyde, Glasgow, G1 1XW, UK (e-mail: david.infield@eee.strath.ac.uk).

This article has been accepted for publication in a future issue of this journal, but has not been fully edited. Content may change prior to final publication. Citation information: DOI 10.1109/TSTE.2018.2884699, IEEE Transactions on Sustainable Energy

speed bin i. All information about the distribution of these N_i points is lost, such as the distribution width (narrow or broad) of the data. The distribution of the data can provide valuable information about the condition of the wind turbine. The abnormal changes to the distribution of the data are usually an indicator of abnormal wind turbine operation.

(2) The bins method only reflects the relationship between wind speed and power output. Other factors which are known to influence the power output are not considered, such as the yaw and pitch systems, and external factors such as wind shear and turbulence. The binned power curve cannot reflect the variation of power output caused by such diverse factors. The modeling accuracy of the bins method will be compared with the new method proposed in section 3.2.

III. Multivariable Gaussian Process (GP) Power Curve Modeling

A. Variable selection for power curve model

The purpose of power curve modeling is to identify the dependency of the wind turbine power output on the key influential factors, including but not restricted to wind speed, when the wind turbine is operating normally, in the absence of any pronounced faults. The power curve model identified will be used as baseline against which to judge whether the wind turbine condition is becoming abnormal in the next monitoring stage.

In this paper, two test wind turbines from a wind farm located in China's Anhui province will be studied. In order to construct a power curve model, it should be determined which factors have a significant influence on power output so that they can be used as model input. The SCADA system of wind turbine records data every 10 minutes. Each record has 29 variables covering different components' sensors. Variables in the SCADA record which have direct impact on the power capture ability should be chosen as the input of the power curve model.

(1) Wind speed and wind direction of the wind resources. Wind is the "fuel" of a wind turbine. Wind speed and direction are the two most important characteristics of the wind resource. Because the test wind farm is located in the mountainous area of Anhui province, when the wind direction changes, the turbulence intensity fluctuates due to a combination of topography and wake effects for particular wind turbines and wind directions, there is a direct impact on their power output.

(2) Pitch angle of the blade pitch system. A large scale wind turbine usually has two different operational regimes. When wind speed is below the rated wind speed, the pitch angle of the blades is kept at or near zero degrees in order to optimize energy capture. When the wind speed is above the rated wind speed, the pitch angle will increase towards 90 degree to reduce the aerodynamic toque so that the power output can be kept at the rated power. The variation of the pitch angle will directly change the attack angle of the wind on the blade changing its aerodynamic efficiency and thus controlling torque and power output. Due to this direct impact, blade pitch angle is chosen as an input to the model.

(3) Yaw error. There is a wind vane on top of the nacelle which measures the wind direction relative to the nacelle direction; this is the yaw error q. When the yaw error exceeds some set value (such as 10 degrees) for some minimum time (such as 60 seconds), the yaw system will turn the rotor and nacelle to minimize the yaw error and keep the rotor normal to the wind. But because of the rapid changes of wind direction and the slow response of the yaw system to limit loads, the yaw error cannot decrease to zero. Associated with yaw error q there is a loss of power, given approximately by:

$$P_q = \cos^3(q) P_0 \tag{1}$$

where, P_0 is the power output when the yaw error is zero.

(4) Rotor speed and tip speed ratio. Besides the wind resource, pitch system and yaw system, the control system of wind turbine plays an important role in trying to optimize wind energy capture. Below rated wind speed, the wind turbine works in Maximum Power Point Tracking (MPPT) mode. In order to produce maximum aerodynamic torque at different wind speeds, the control system will regulate the electromagnetic torque of the generator to adjust the rotor speed so that the relative wind velocity which is the vectorial composition of blade rotating speed and wind speed impinges on the blade at the desired attack angle. As a result, the rotor speed will increase when the wind speed is high and vice versa. There is a parameter called tip speed ratio l which is the ratio of the velocity of the blade tip to the wind speed:

$$l = \frac{wR}{V} \tag{2}$$

where, w is the rotor angular velocity; R is the radius of the rotor, and V is the wind speed. The tip speed ratio determines the aerodynamic efficiency of the rotor and how near this is to its optimal value reflects the performance of the control system. When the tip speed ratio is near its optimal value, the wind energy capture efficiency of wind turbine is high. Otherwise under some conditions, such as the poor control performance or when the control parameter mismatches the local wind resource, the tip speed ratio can deviate far away from the optimal value which will result in the wind turbine poor power generation performance. As the parameters of the control system, rotor speed and tip speed ratio should be included as inputs to the power curve model.

Following aerodynamic energy capture by the rotor, the drive train and generator finally convert the mechanical energy into electricity. The energy losses of these components (the drive train, generator) are usually small and fairly constant, so that the parameters related to these components don't have an obvious impact on the wind turbine power output characteristics. For the test wind turbine in this paper, when the gearbox temperature is higher than 80 ^{o}C or the generator stator temperature is higher than 150 ^{o}C for more than 60 seconds, the wind turbine will shut down automatically. Shutdowns caused by these conditions may decrease the energy production of the wind turbine, but this only affect the

This article has been accepted for publication in a future issue of this journal, but has not been fully edited. Content may change prior to final publication. Citation information: DOI 10.1109/TSTE.2018.2884699, IEEE Transactions on Sustainable Energy

power output characteristics slightly, and can be excluded from the data sets analyzed. When the temperature decreases to below 80 ^{o}C and 150 ^{o}C for the gearbox and the generator respectively, the wind turbine will restart.

As mentioned above, the wind resource, pitch system, yaw system and control system will directly affect the wind energy capture ability of wind turbine. As a result, the wind speed and direction, pitch angle, yaw error, rotor speed and tip speed ratio are chosen as inputs to the power curve model input. And the output of the model is power output prediction.

B. Multivariable Gaussian Process (GP) power curve modeling and validation

For any wind turbine, the working condition is constantly changing. With the variation of the wind speed, parameters such as rotor speed, pitch angle, and power output will change, to an extent randomly. The SCADA data for a wind turbine exhibits strong stochastic characteristics. Gaussian Process modeling is a Bayesian method which has good performance with stochastic data, [9-11].

A Gaussian Process is completely specified by its mean value $m(\boldsymbol{x})$ and covariance function $k(\boldsymbol{x}, \boldsymbol{x}')$ and can be written as:

$$f(\boldsymbol{x}) \sim GP\big(m(\boldsymbol{x}), k(\boldsymbol{x}, \boldsymbol{x}')\big) \tag{3}$$

Assume that there are already N data points $(\boldsymbol{X}, \boldsymbol{y})$, $\boldsymbol{X} = \{\boldsymbol{x}_1, \mathbf{L}, \boldsymbol{x}_i, \mathbf{L}, \boldsymbol{x}_N\}$, $\boldsymbol{y} = \{y_1, \mathbf{L}, y_i, \mathbf{L}, y_N\}$. For a new data point with input $\boldsymbol{x}_*$ and unknown predicted output y_* with same distribution, by conditioning the joint Gaussian prior distribution on the existing data $(\boldsymbol{X}, \boldsymbol{y})$, the posterior probabilistic distribution is obtained as:

$$y_* \mid \boldsymbol{X}, \boldsymbol{y}, \boldsymbol{x}_* \sim N(\bar{y}_*, s_*^2) \tag{4}$$

where, $\bar{y}_* = \boldsymbol{K}(\boldsymbol{x}_*, \boldsymbol{X})\boldsymbol{K}^{-1}(\boldsymbol{X}, \boldsymbol{X})\boldsymbol{y}$ is the mean predicted value of y_*, and

$s_*^2 = \boldsymbol{K}(\boldsymbol{x}_*, \boldsymbol{x}_*) - \boldsymbol{K}(\boldsymbol{x}_*, \boldsymbol{X})\big[\boldsymbol{K}(\boldsymbol{X}, \boldsymbol{X}) + s_n^2 \boldsymbol{I}\big]^{-1}\boldsymbol{K}(\boldsymbol{X}, \boldsymbol{x}_*)$ is the variance of the prediction y_*.

In this paper, the squared exponential is used as the covariance function. Its matrix form is:

$$\boldsymbol{K}(\boldsymbol{x}_i, \boldsymbol{x}_j) = s_f^2 \exp\left[-\frac{1}{2}\big(\boldsymbol{x}_i - \boldsymbol{x}_j\big)^{\mathrm{T}} \boldsymbol{D}\big(\boldsymbol{x}_i - \boldsymbol{x}_j\big)\right] + s_n^2 \boldsymbol{\delta}_{ij} \tag{5}$$

where the hyperparameters are $\Theta = \{s_f^2, \{\boldsymbol{D}\}, s_n^2\}$, s_f^2 is the signal variance and s_n^2 is the noise variance. $\boldsymbol{D} = \mathrm{diag}(d_1, d_2, \mathbf{L}, d_L)$ is the length scale parameter for each of the model inputs which links the time variation of the input parameter to that of the output.

The conjugate gradient method and data points $(\boldsymbol{X}, \boldsymbol{y})$ are used to maximize the marginal likelihood to get the final value of hyperparameters. During the process, the large scale covariance matrix $\boldsymbol{K}$ must be inverted and the computational demands are significant if the dimension is high. In this paper, a Cholesky decomposition is used to compute $\boldsymbol{K}^{-1}$ since it is fast and numerically stable. Because the covariance matrix $\boldsymbol{K}$ is a positive definite matrix, there is a lower triangular matrix $\boldsymbol{L}$ which makes $\boldsymbol{K} = \boldsymbol{L}\boldsymbol{L}^{\mathrm{T}}$ and $\boldsymbol{L} = \mathrm{cholesky}(\boldsymbol{K})$. $\boldsymbol{L}$ is Cholesky factor. With Cholesky decomposition, the inversion of matrix $\boldsymbol{K}$ can be computed as:

$$\boldsymbol{K}^{-1} = \big(\boldsymbol{L}^{\mathrm{T}}\big)^{-1} \times \boldsymbol{L}^{-1} \tag{6}$$

The predicted value of Gaussian Process becomes:

$$\bar{y}_* = \boldsymbol{K}(\boldsymbol{x}_*, \boldsymbol{X})\boldsymbol{K}^{-1}(\boldsymbol{X}, \boldsymbol{X})\boldsymbol{y} = \boldsymbol{K}(\boldsymbol{x}_*, \boldsymbol{X})\big(\boldsymbol{L}^{\mathrm{T}}\big)^{-1}\boldsymbol{L}^{-1}\boldsymbol{y} \tag{7}$$

The computational complexity of Cholesky decomposition is much smaller than that of the conventional matrix invertion. With the Cholesky decomposition, the Gaussian Process power curve modeling can be quickly and accurately.

The SCADA data from test wind turbine 1 (denoted E16) during the period 26/04/2017 to 25/05/2017 is used for power curve modeling and validation. The original data has 4320 10-minute records. After removing the records covering the wind turbine stop period and bad records caused by the start and stop process (the power output is obviously much lower than others at the same wind speed), there remains 3643 records. Wind speed and direction, pitch angle, yaw error, rotor speed and power output are selected from each record and the tip speed ratio computed using (2). These seven variables together make up one sample. Power output is used as the model output, and the other six are used as model inputs. There are in total 3643 samples. For good modeling accuracy, the seven variables in the samples must be normalized before being used for modeling. This is done using the ranges given in TABLE I.

TABLE I
Parameters for Variable Normalization

Variable	Unit	Lower Limit	Upper Limit
Wind speed	m/s	2	20
Wind direction	degree	0	359
Pitch angle	degree	0	30
Yaw error	degree	-60	60
Rotor speed	rpm	10	18
Tip speed ratio	--	0	25
Power output	KW	0	1600

After normalization, the first 3143 samples are used for Gaussian Process power curve modeling, leaving 500 samples for model validation. With 3143 samples and the Cholesky decomposition for matrix inversion and conjugate gradient method, the hyperparameters for the Gaussian Process power curve model are determined; these are given in TABLE II. The model construction is now complete. With hyperparameters and (7), the power curve model can give power output predictions for new inputs.

TABLE II
Hyperparameters for Gaussian Process Power Curve Model

s_f^2	s_n^2	Wind speed	Wind direction	Pitch angle	Yaw error	Rotor speed	l
0.228	0.005	29.05	2.41	36.0	4.97	6.38	7.55

Using the 500 samples reserved for validation as input to the power curve model, the results are shown in Fig.1, together

This article has been accepted for publication in a future issue of this journal, but has not been fully edited. Content may change prior to final publication. Citation information: DOI 10.1109/TSTE.2018.2884699, IEEE Transactions on Sustainable Energy

with the model residuals. The residuals are generally less than 10%.

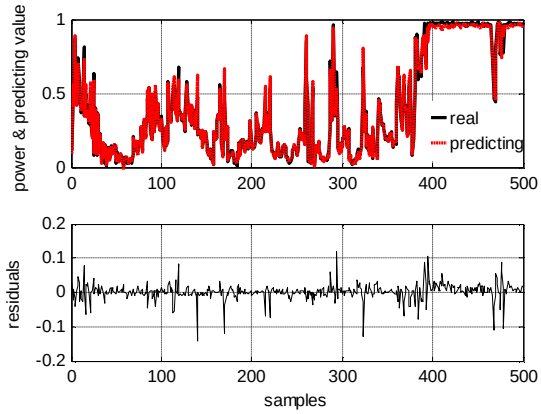

Fig.1 Validation for GP power curve model (normalized values)

In order to show the result more clearly, we transform the normalized power output and its predicted values to their real value range of 0-1600KW and plot them in the conventional way in Fig.2.

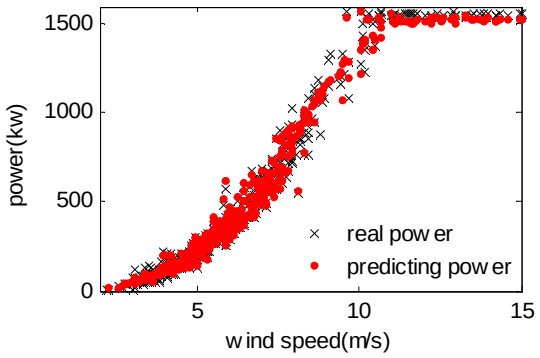

Fig.2 Validation for GP power curve model

In order to compare with GP power curve model above, two other power curve modeling method the binned method and the sixth order polynomial regression method in [6] are studied. With the same 3143 samples, the power curve modeling results of the binned method and sixth order polynomial regression method are shown in Fig.3.

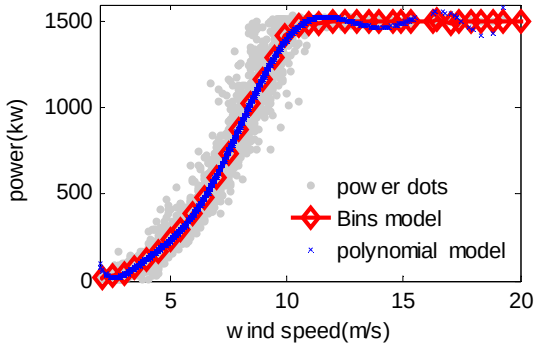

Fig.3 Bins and sixth order polynomial regression power curve models

In Fig.3, the binned model comprises 36 mean power and wind speed points between 2 and 20 m/s. These points are connected by lines to form the power curve. The sixth order polynomial regression model is:

$$y = -140.05x^6 + 408.90x^5 - 434.39x^4 + 199.48x^3 - 36.41x^2 + 3.49x - 0.08 \quad (8)$$

Where, y is the power and x is the wind speed.

The binned and sixth order polynomial regression power curve models can be used to predict the power output for the validation data set. For the binned method, the predicted power output is obtained by interpolating appropriately between the binned wind speed values. The predicting results for these two power curve model are shown in Fig.4.

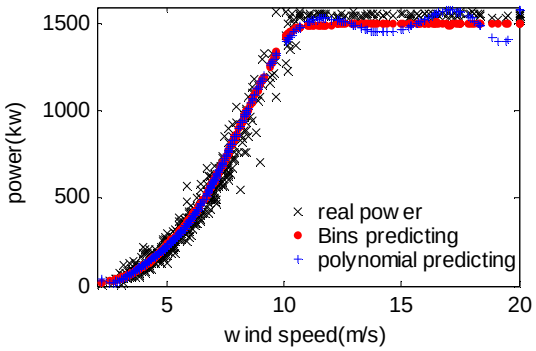

Fig.4 Validations for bins and sixth order polynomial regression power curve models

Mean absolute percentage error (MAPE) is calculated for these three power curve models' validating accuracy in Fig.2 and Fig.4 as TABLE III.

$$\mathrm{MAPE} = \frac{1}{N}\sum_{i=1}^{N}\frac{|y_i - \hat{y}_i|}{y_i}\cdot 100\% \quad (9)$$

Where, y_i is the real power in validation data, and $\hat{y}_i$ is the model predicting power.

TABLE III
MAPE for Three Power Curve Modeling Methods

Modeling Method	MAPE
Method of Bins	11.83%
Sixth order polynomial regression	12.06%
Multivariable GP method	5.87%

In Fig.4, because the binned method and the sixth order polynomial regression method only use the wind speed as model input, their predicted power outputs form a "line" shape without variation. The MAPEs for these two methods are quite similar as 11.83% and 12.06% respectively.

In contrast, in Fig.2, we can see that the predicted power outputs from the GP model are scattered to form a "band" in much the same way as the measurements, reflecting the impact of variables other than wind speed. And the MAPE for GP model is 5.87% which is quite smaller than the two other power curve models. The multivariable GP power curve modeling method has significantly improved modeling accuracy.

IV. Sequential Probability Ratio Test (SPRT) Residual Analysis and Power Curve Monitoring

A. SPRT residual analysis

As shown above, the multivariable GP power curve model

This article has been accepted for publication in a future issue of this journal, but has not been fully edited. Content may change prior to final publication. Citation information: DOI 10.1109/TSTE.2018.2884699, IEEE Transactions on Sustainable Energy

has good modeling accuracy and can describe the dependency of power output on key input factors when the wind turbine works normally. Thus the GP power curve can be used as a baseline to monitor the wind turbine working condition and provide alarms when abnormal operation occurs. When the wind turbine works normally, the GP power curve model will give an accurate prediction of the real power output and the residuals between real and predicted power will be small. When the wind turbine encounters faults, the relationship between the power and the input factors will deviate from the model, which will result in the model's prediction residuals become larger. Careful assessment of the residuals can deliver alarms in an accurate and timely way.

In this paper, a Sequential Probability Ratio Test (SPRT) is used to detect any abnormal changes to the GP power curve residuals. Fig.5 shows the GP power curve monitoring procedure.

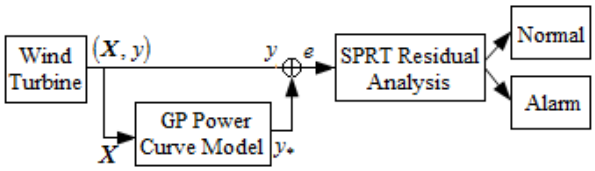

Fig.5 GP power curve monitoring procedure

The SPRT is a statistical technique developed by Wald [12-14]. SPRT consists of two possible testing hypotheses. Hypotheses H_0: the wind turbine is fault free and the model residuals have a normal distribution with mean value m_0 and variance s_0^2; Hypotheses H_1: the wind turbine exhibits abnormal operation with the mean value and variance of the model residuals respectively changing to m_1 and s_1^2 respectively. For the GP power curve model residual sequence $e_1, e_2, \mathbf{L}, e_n$, the joint probability densities for H_0 and H_1 are respectively as follows.

$$P_{0n} = \frac{1}{\left(s_0\sqrt{2p}\right)^n}\exp\left(-\frac{1}{2s_0^2}\sum_{i=1}^{n}(e_i - m_0)^2\right) \quad (10)$$

$$P_{1n} = \frac{1}{\left(s_1\sqrt{2p}\right)^n}\exp\left(-\frac{1}{2s_1^2}\sum_{i=1}^{n}(e_i - m_1)^2\right) \quad (11)$$

The SPRT ratio (or the likelihood ratio) is:

$$R_m = \frac{P_{1n}}{P_{0n}} \quad (12)$$

The false alarm probability and missed alarm probability respectively are set as a and b which give a lower limit A and an upper limit B respectively as:

$$A = \frac{b}{1-a},\ B = \frac{1-b}{a}. \quad (13)$$

If $R_m \le A$, hypothesis H_0 should be accepted and the wind turbine is regarded as operating normally. Conversely, if $R_m \ge B$, hypothesis H_0 should be rejected H_1 accepted instead and the wind turbine operation is regarded as abnormal, triggering an alarm. If neither of these two limits is reached, the current information is not sufficient to make a conclusion and the sampling continues. The simple log form of the SPRT ratio is used here:

$$\ln R_m = n\ln\left(\frac{s_0}{s_1}\right) + \left(-\frac{1}{2s_1^2}\sum_{i=1}^{n}(e_i - m_1)^2 + \frac{1}{2s_0^2}\sum_{i=1}^{n}(e_i - m_0)^2\right) \quad (14)$$

with $\ln R_m$ compared with $\ln A$ and $\ln B$ to provide the turbine health status.

In reality, when an abnormality occurs, the mean value of the residuals may increase or decrease and shifts from the m_0 to m_1 as $m_0 + \Delta m$ or $m_0 - \Delta m$. In order to cover these two situations, two group hypotheses are proposed:

Group 1: H_0 and H_{1A} with mean value $m_0 + \Delta m$ and variance s_1^2, and the SPRT ratio for H_0 and H_{1A} is R_{m1}.

Group 2: H_0 and H_{1B} with mean value $m_0 - \Delta m$ and variance s_1^2, and the SPRT ratio for H_0 and H_{1B} is R_{m2}.

In the wind turbine monitoring stage, R_{m1} and R_{m2} are computed at the same time and compared with the upper and lower limit to determine alarms. For the test wind turbines in this paper, $a = b = 0.05$ and the parameters for H_0, H_{1A} and H_{1B} are shown in TABLE IV.

TABLE IV
Parameters for Hypotheses

Hypotheses	Description	mean value	variance
H_0	Working normally	m_0	s_0^2
H_{1A}	Abnormal (mean value increasing)	$m_0 + 3m_0$	$1.5\,s_0^2$
H_{1B}	Abnormal (mean value decreasing)	$m_0 - 3m_0$	$1.5\,s_0^2$

The mean value and variance of H_0 can be obtained from the residuals of the validation samples.

B. The location of the failed components which caused the alarms

If the SPRT generates an alarm, it means that the wind turbine behavior has changed from the GP power curve model of the healthy turbine, and performance degradation has occurred. It is important to find out which components lead to this loss of performance so as to give the wind farm operator information to guide the required repair.

As mentioned in 3.1, the wind resource, pitch system, yaw system and control system all significantly affect the wind turbine energy capture ability. When an alarm is generated by GP power curve model and SPRT method, attention should be paid to check the working condition of these systems. In order of importance, the following should be checked: (1) wind anemometer and vane; (2) checking blade surface condition whether there is blade surface cracking or ice accumulation (e.g. using an unmanned aerial vehicle); (3) pitch actuator, pitch angle of each blade and the mean pitch angle of the three blades; (4) Yaw actuator and yaw error; (5) the rotor speed

This article has been accepted for publication in a future issue of this journal, but has not been fully edited. Content may change prior to final publication. Citation information: DOI 10.1109/TSTE.2018.2884699, IEEE Transactions on Sustainable Energy

and tip speed ratio control. There are two methods to check whether a component has failures: (1) compare the components' operating data before and after the alarm to identify possible differences. This approach can be considered as a longitudinal data comparison of the turbine in question. See reference [4] as an example of this method; (2) compare the components' operating data for the turbine highlighted by the alarm with the data from nearby healthy turbines which are seeing a similar wind resource due to proximity. This approach can be described as a transverse data comparison between different wind turbines.

In the case of a direct-drive wind turbine with a Permanent Magnet Synchronous Generator (PMSG) and fully rated converter, some type of converter faults, such as an open-circuit fault in an IGBT of the grid-side converter, will also decrease the wind turbine power output and performance [15]. The converter current must be used as the diagnostic parameter with a quite high sampling rate (millisecond) which cannot be achieved by SCADA system. A specially designed converter condition monitoring system is needed instead of the SCADA data comparison method proposed in this paper [16-17].

C. Industrial study cases

In this section, industrial cases associated with two 1.5MW DIFG test wind turbines located in China Anhui province are studied. Fig.6 is the satellite picture of the test wind turbines and wind farm.

Fig.6 Satellite view of the test wind turbines

These two wind turbines both experienced abnormal operation due to documented component failures. The data for test wind turbine 1 (denoted E16) was obtained during the period 25/04/2017 to 15/06/2017. Data from wind turbine 2 (denoted P01) was taken from 08/05/2017 to 24/06/2017. The relationship between power output and wind speed for E16 and P01 are shown in Fig.7 and Fig.8 respectively. In these two figures, data points in black-dot represent wind turbines work in healthy condition while the red-cross points are data when wind turbines encounter faults.

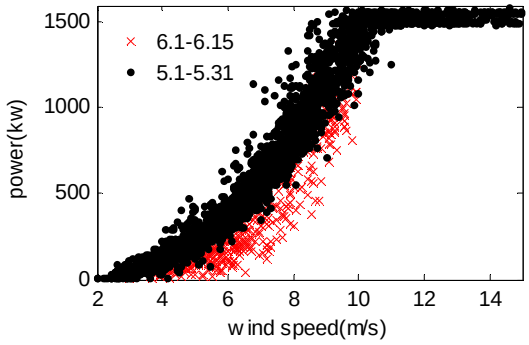

Fig.7 Data from wind turbine 1 (E16)

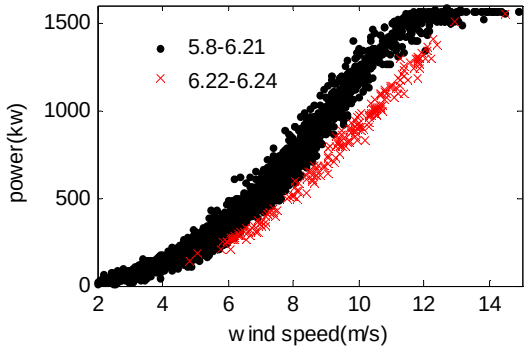

Fig.8 Data from wind turbine 2 (P01)

Study Case 1

Test wind turbine 1 (E16) was studied in the section 3.2. After the GP power curve model was constructed and validated, operating data from 26/05/2017 to 05/06/2017 was used as monitoring data. After preprocessing the data (to remove any stop-time data and for data normalization), the first 1000 samples of this period are used for the GP power curve model with the predicted values and residuals as shown in Fig.9.

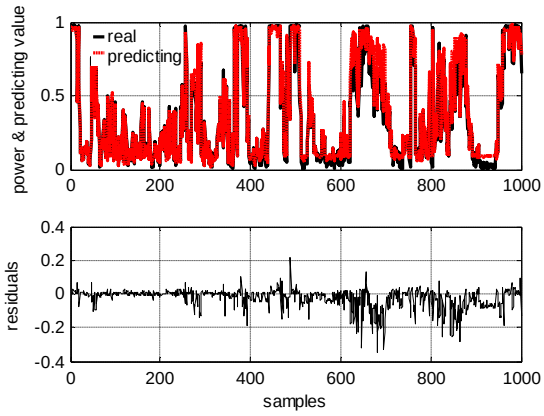

Fig.9 Monitoring results from GP model for E16

In Fig.9, the model residuals are small initially, but then grow becoming increasingly negative.

SPRT, as in 4.1, is used to analyze the residuals shown in Fig.9 for turbine E16. The mean value m_0 and variance s_0^2 are computed with the 500 residuals of Fig.1. The SPRT monitoring result is shown in Fig.10.

This article has been accepted for publication in a future issue of this journal, but has not been fully edited. Content may change prior to final publication. Citation information: DOI 10.1109/TSTE.2018.2884699, IEEE Transactions on Sustainable Energy

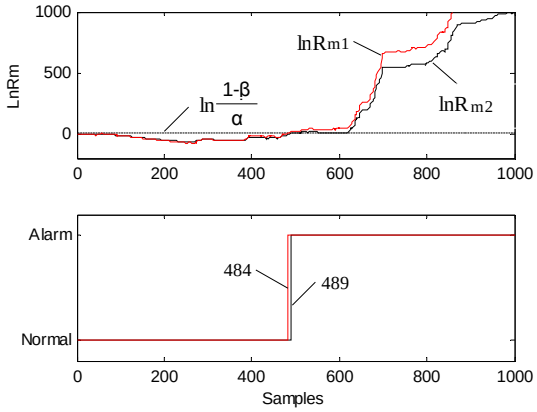

Fig.10 SPRT alarm status for turbine E16

By comparing Fig.9 and Fig.10, it can be seen that the SPRT is sensitive to changes in the residuals. At point 484 and point 489, the log SPRT ratios $\ln R_{m1}$ and $\ln R_{m2}$ for hypotheses group1 and group2 respectively reach the upper limit and generate alarms. Tracing back to original operating data, the alarm points 484 and 489 in Fig.10 are respectively at 16:00 and 16:50 on 01/06/2017.

In order to locate the component causing the alarm, the methods outlined in 4.2 are used. Another wind turbine, E17, geographically near turbine E16 is selected for a transverse analysis. Fig.11 shows the wind speed data for these two wind turbines during the period 02/05/2017 to 30/06/2017.

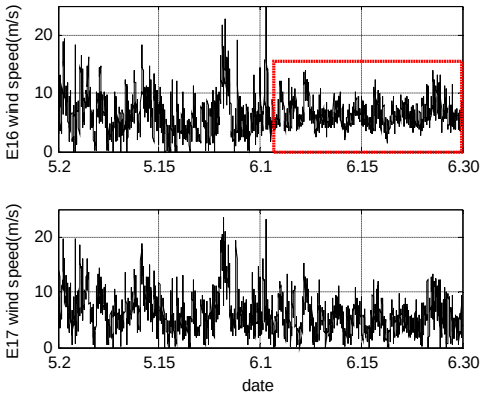

Fig.11 Transverse comparison of wind speed between E16 and E17

From the transverse comparison of wind speed between E16 and E17, we can see that before the alarm date of 01/06/2017, the wind speeds of E16 and E17 are quite similar, while after 01/06/2017, there is no wind speed lower than 2m/s recorded at turbine E16. We infer that there is an erroneous systemic increase of the wind speed as measured by the E16 anemometer during low winds.

The GP power curve model with SPRT detects the abnormality of test wind turbine 1 (E16) in a fast and effective manner. Following the alarm, the transverse data comparison method enables anemometer failure on E16 to be identified as the cause of the wind turbine's abnormal performance.

Study case 2

SCADA data from wind turbine 2 (P01) during the period 08/05/2017 to 18/06/2017 is used as model and validation data for the GP power curve model. The procedure is same as for turbine 1 (E16) and does not merit detailed discussion here.

The SCADA data from 19/06/2017 to 24/06/2017 are used as monitoring data for P01 after preprocessing as previously described. The first 500 monitoring samples are used as input to the GP power curve model and the monitoring results are shown in Fig.12.

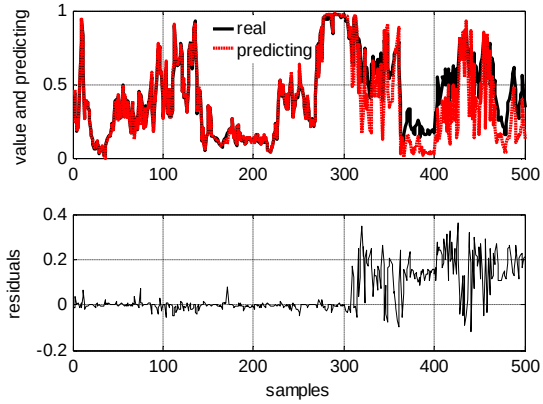

Fig.12 Monitoring results for GP power curve model of P01

The SPRT residual analysis is shown in Fig.13.

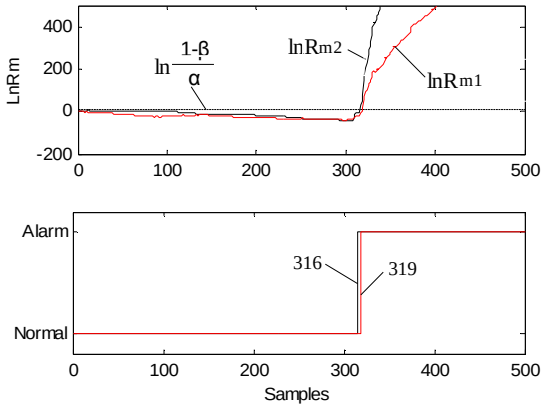

Fig.13 SPRT alarm status for wind turbine P01

Comparing Fig.12 and Fig.13, we can see that at points 316 and 319, log SPRT ratios $\ln R_{m2}$ and $\ln R_{m1}$ reach the upper limit and alarms are triggered. The alarm points 316 and 319 are data at 3:50 and 4:20 on 22/06/2017.

Following the alarms, as before, the reason for abnormal performance should be identified. Using the longitudinal data comparison method of 4.2, it is found that the pitch system is operating poorly.

This article has been accepted for publication in a future issue of this journal, but has not been fully edited. Content may change prior to final publication. Citation information: DOI 10.1109/TSTE.2018.2884699, IEEE Transactions on Sustainable Energy

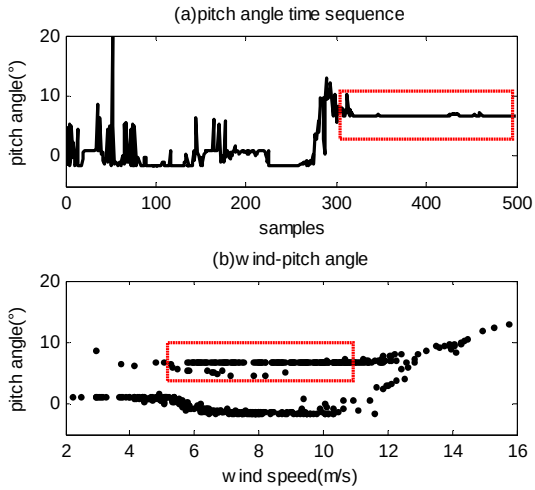

Fig.14 Pitch angle for data for wind turbine P01

From Fig.14 (a) it is clear that a pitch control problem has developed: from point 311 the pitch angle remains constant at 6.6 degrees. Fig.14 (b) confirms this because below rated wind speed the pitch angle should be near zero while clearly there is significant data showing a pitch angle of 6.6 degrees, as in the red-dash line rectangle.

Again it is shown that the GP power curve model together with SPRT generate alarms in a timely manner. Using the longitudinal data comparison method, blade pitch control failure is found to be the reason for abnormal performance.

D. SPRT Discussion

In the above two study cases, it is useful to study which log SPRT ratios, $\ln R_{m1}$ or $\ln R_{m2}$, reaches the upper limit later and the changing direction of the mean value of residuals after the fault.

(1) In study case 1, because of the fault with the anemometer system, the measured wind speed is higher than the real wind speed. As a result, the GP power curve model gives a higher power prediction than the real power output and the residuals in Fig.9 decrease and move to the minus direction. In Fig.10, the second group hypotheses in which H_{1B} correctively assumes that the mean value decreases alarms later than the first group hypotheses in which H_{1A} wrongly indicates that the mean value increases by 5 points ($\ln R_{m2}$ at 489 and $\ln R_{m1}$ at 484).

(2) In study case 2, because of the blade pitch angle gets stuck at 6.6 degrees when it should be at zero, and because pitch angle has a major impact on power output, the GP power curve model greatly decreases the power output prediction which results in the predicted power being significantly lower than the real power. As a result, the residuals in Fig.12 increase and move obviously into the positive direction. In Fig.13, the first group hypotheses in which H_{1A} correctively assumes an increasing mean value alarms later than the second group hypotheses in which H_{1B}'s assumption is wrong by 3 points ($\ln R_{m1}$ at 319 and $\ln R_{m2}$ at 316).

With these two study cases, we can see that the log SPRT ratios of hypotheses which correctively assume the mean value changing direction (i.e. the assumption is consistent with the real residual changing direction) reach the upper limit and alarm later than the contrary hypotheses. The phenomenon can be explained since the former can provide a greater margin for safety and must wait for a bigger SPRT ratio and more abnormal samples to reach the alarm upper limit. Although the contrary hypothesis may trigger alarms more quickly, its safety margin is smaller, which may result in false alarms. As a conclusion, we propose using the later alarm such as point 489 for E16 and point 319 for P01 to inform the operator so as to ensure greater alarm reliability. TABLE V shows the recommended alarm points for the two wind turbines.

TABLE V
Recommended Alarm Points for Test Wind Turbines

Wind turbine	E16	P01
Residual mean value change direction	***Decreasing***	***increasing***
Alarm point for $\ln R_{m1}$ (assuming residual mean value ***increasing***)	484	**319**
Alarm point for $\ln R_{m2}$ (assuming residual mean value ***decreasing***)	**489**	316
Recommended Alarm point	**489**	**319**

V. Conclusions

In this paper, data from two 1.5 megawatt test wind turbines has been used to develop and test an effective fault identification approach based on multivariable GP power curve modeling supported by SPRT for alarm generation. This work supports the following conclusions.

(1) The bins power curve modeling method loses valuable information about the scattering and variation of the data which hold important clues regarding wind turbine abnormal operation and performance degradation.

(2) After carefully selection of the model inputs, a modified Gaussian Process (with Cholesky decomposition) is used to construct the power curve model. Compared with two other modeling methods (the bins and the sixth order polynomial regression), the multivariable GP power curve model is shown to have much higher modeling accuracy.

(3) The SPRT method is introduced to analyze GP model residuals. Two groups of hypotheses are proposed to cover different changes to the mean value. For the two study cases, the SPRT method detects the abnormalities for these two test wind turbines and gives alarms in a highly effective manner.

(4) Two data comparison methods are proposed for location of the faulty components (or subsystems). Following alarms, longitudinal and transverse data comparisons should be undertaken to check the condition of key components.

This paper proposes a hierarchical structure for wind turbine condition monitoring. The higher level comprises wind turbine overall performance monitoring, that is, the power curve modeling and monitoring. The lower level is the condition

This article has been accepted for publication in a future issue of this journal, but has not been fully edited. Content may change prior to final publication. Citation information: DOI 10.1109/TSTE.2018.2884699, IEEE Transactions on Sustainable Energy

monitoring of the key components using longitudinal and transverse data comparison methods. Once abnormalities have been detected at the higher level (the wind turbine power curve encounters notable deviation from normality), the lower level (key components condition monitoring) will be triggered. With the development of such a hierarchy for analysis, wind turbine condition monitoring can be better automated.

REFERENCES

[1] *Power performance measurements of electricity producing wind turbines*, IEC 61400-12-1, 2005.

[2] M. Lydia, S. Suresh Kumar, A. Immanuel Selvakumar, G. Edwin Prem Kumar, "A comprehensive review on wind turbine power curve modeling techniques", *Renewable and Sustainable Energy Reviews*, Vol. 30, pp. 452-460, 2014.

[3] Vaishali Sohoni, S.C.Gupta, R.K.Nema, "A critical review on wind turbine power curve modeling techniques and their applications in wind based energy systems", *Journal of Energy*, Vol. 2016, pp. 1-18, Jun. 2016.

[4] Andrew Kusiak, Haiyang Zheng, Zhe Song, "On-line monitoring of power curve", *Renewable Energy*, Vol. 34, no. 6, pp. 1487-1493, 2009.

[5] Andrew Kusiak, Anoop Verma, "Monitoring wind farms with performance curves", *IEEE Trans. on Sustainable Energy*, Vol. 4, no. 1, pp. 192-199, Jan. 2013.

[6] Mantas Marciukaitis, Inga Zutautaite, Linas Martisauskas, etc, "Non-linear regression model for wind turbine power curve", *Renewable Energy*, Vol. 113, pp. 732-741, 2017.

[7] Han Huali, Zhang Genbao, Yang Wei, "Influence and adjustment of turbulence intensity on measured power curve of wind turbine", *Acta Energiae Solaris Sinica*, Vol. 36, no. 6, pp. 1442-1447, Jun. 2015.

[8] Mingdi You, Bingjie Liu, Eunshin Byon, etc, "Direction-dependent power curve modeling for multiple interacting wind turbines", *IEEE Trans. on Power Systems*, Vol.33, no. 2, pp. 1725-1733, Mar. 2018.

[9] Rasmussen C.E., Christopher K.I, *Gaussian Processes for Machine Learning*, Massachusetts: The MIT Press, 2005, pp. 7-31.

[10] Niya Chen, Zheng Qian, Ian T. Nabney, Xiaofeng Meng, "Wind power forecasts using Gaussian Processes and numerical weather prediction", *IEEE Trans. on Power Systems*, Vol.29, no.2, pp. 656-664, Mar. 2014.

[11] Jianming Hu, Jianzhou Wang, "Short-term wind speed prediction using empirical wavelet transform and Gaussian process regression", *Energy*, Vol. 93, part 2, pp. 1456-1466, 2015.

[12] Chenzong Bai, Vijay Gupta, "An on-line sensor selection algorithm for SPRT with multiple sensors", *IEEE Trans. on Automatic Control*, Vol. 62, no. 7, pp. 3532-3539, Jul. 2017.

[13] Wang Rong, Xiong Zhi, Liu Jianye, Xu Jianxian, Shi Lijuan, "Chi-square and SPRT combined fault detection for multisensory navigation", *IEEE Trans. on Aerospace and Electronic Systems*, Vol. 52, no. 3, pp. 1352-1365, Jun. 2016.

[14] R. Satya Prasad, Srisaila, G. Krishna Mohan, "Software reliability using SPRT: power law process model", International Journal of Electronics and Computer Science Engineering, Vol. 3, no. 4, pp. 446-454, 2015.

[15] Jorge O. Estima, Jose L.J. Fernandes, A.J.Marques Cardoso. "Faulty operation analysis of permanent magnet synchronous generator drives for wind turbine applications", in *Proc. 5th IET Int. Conf. Power Electronics, Machines and Drives*, Brighton, UK, Apr. 2010,

[16] Imed Jlassi, Jorge O. Estima, Sejir Khojet E. K., Najiba Mrabet Bellaaj, Antonio J. Marques Cardoso. "Multiple open-circuit fault diagnosis in back-to-back converters of PMSG drives for wind turbine systems", *IEEE Transactions on Power Electronics*, vol.30, no. 5, pp. 2689-2702, 2015.

[17] Keyuan Huang, Weixing Yang, Li Wang, Shoudao Huang. "Open-circuit fault diagnosis of single converter device for directly-driven wind power system", *in Proc. 17th Int. Conf. Electrical Machines and Systems*, Hangzhou, Oct. 2015.

BIOGRAPHIES

Peng Guo was born in Hebei, China in June 1975. He received the Ph. D. degree from the North China Electric Power University, Beijing, China, in 2004, and the B.S and M.S degrees from the North China Electric Power University, Baoding City, China, in 1998 and 2001, respectively. He is a professor of the School of Control and Computer Engineering, North China Electric Power University since 2014. His research interests include wind turbine condition monitoring, SCADA data analysis and control.

David Infield (SM'2007) was born in Paris, France in 1954 and raised and educated in England. He is now Professor of Renewable Energy Technologies with the Institute of Energy and Environment within the Department of Electronic and Electrical Engineering at the University of Strathclyde, Glasgow, UK. He is Editor in Chief of the IET journal Renewable Power Generation, and contributes to various IEC, CENELEC and IPPC activities.